Multicritical Phenomena and Microphase Ordering in Random Block Copolymer Melts

Glenn H. Fredrickson*

Department of Chemical & Nuclear Engineering and Materials Department, University of California, Santa Barbara, California 93106

Scott T. Milner

Exxon Research and Engineering Company, Annandale, New Jersey 08801

Ludwik Leibler

Laboratoire de Physico-Chimie Theorique, ESPCI, 75231 Paris Cedex 05, France

Received February 21, 1992; Revised Manuscript Received July 6, 1992

ABSTRACT: A mean-field analysis of microphase separation and phase behavior is described for melts of linear A–B multiblock copolymers, each chain consisting of a stochastic sequence of flexible segments (each with M monomers), A_M and B_M, for a total of $Q \gg 1$ segments per chain. We find a phase diagram similar to that for statistical A–B copolymers ($M = 1$) but with an isotropic Lifshitz point that should be accessible for a wide variety of materials. Due to the broad distribution of sequence lengths of like monomers, the microphases are predicted to lack long-range order and to exhibit unusual temperature sensitivity at the order–disorder transition. This may open the way to a novel class of polyurethanes and thermoplastic elastomers.

I. Introduction

In recent years there has been a flurry of experimental and theoretical work aimed at developing an understanding of model copolymeric materials with well-defined architectures.[1-5] Such systems include simple diblock and triblock copolymers but also more complex star or graft block copolymers, usually prepared by anionic polymerization techniques. Considerable attention, both theoretical[6-11] and experimental,[12-14] has also been given to regular (alternating) $(AB)_n$ multiblock copolymers. The interest in such materials stems from their widespread applications as adhesives, emulsifiers, barrier materials, and impact modifiers.

Crucial to many of these applications is the dramatic change in mechanical properties of block copolymers as they pass through the so-called microphase separation transition or order–disorder transition (ODT),[2,15] at which blocks of different chemical composition segregate to form microdomains, producing a spatially inhomogeneous composition pattern throughout the material. In systems with a relatively narrow distribution of block lengths and topologies of connections, i.e., well-defined architectures, it is typically the case that the composition patterns (or "microphases") achieve long-range or quasi-long-range order upon annealing. Depending upon the composition and particular architecture of the copolymer, body-centered-cubic arrays of spheres, hexagonal arrays of cylinders, ordered-bicontinuous-double-diamond, and lamellar phases have all been observed.[1-5] The mechanical properties of a copolymeric material can depend sensitively on which of these ordered microphases is actually present.

It is now well established in model A–B block copolymer systems, such as anionically prepared diblocks, that there exist large-amplitude composition fluctuations in the pretransitional disordered phase of a copolymer melt.[2] These fluctuations are manifested in small-angle neutron scattering (SANS) experiments as a broad correlation hole peak in the structure factor, whose position q^* changes only weakly with temperature as the ODT is traversed. There are essentially only two block lengths (N_A and N_B) in such materials; hence, the spatial length scale for composition fluctuations and (below the transition) microphases, $D = 2\pi/q^*$, reflects a combination of the radii of gyration of these two blocks, R_A and R_B. Aside from a weak extension of the blocks' radii from their unperturbed (Gaussian) dimensions due to polarization by the inhomogenous medium,[16,17] q^* is approximately constant in the transition region in accordance with theory.[15] Complementary dynamical mechanical measurements[18] on A–B diblocks indicate that, apart from an abrupt change in the shear modulus at the ODT, the ordered-phase modulus does not exhibit any unusual or rapid variation with temperature. At much lower temperatures, in the so-called strong segregation limit (SSL),[19,20] chains become strongly extended by the chemical forces and the microdomain period D can be significantly larger than the unperturbed values of either R_A and R_B.

A second class of copolymers, which include random (or statistical) copolymers, random multiblock copolymers, and other copolymeric materials of ill-defined architecture or composition, have received much less attention from theorists[6,21,22] and experimental scientists[14,23] yet have tremendous commercial significance and engineering interest. Examples of engineering materials that fall in this category include polyurethanes, SBR rubber, HIPS, and ABS. Recent theoretical studies of random copolymer melts[24-27] have demonstrated that, in spite of the chemical complexity of such systems, tractable thermodynamic calculations can be performed by the use of replica-averaging methods. These calculations have yielded new insights into compositional ordering of random copolymers and have isolated some unusual multicritical behavior under appropriate polymerization conditions.[25] Two particularly striking predictions are that microphases in random copolymer melts will typically lack long-range order and that the microphase period D should exhibit extreme temperature sensitivity near the ODT. Both predictions arise from the broad distribution of monomer sequence lengths present in a random copolymer sample, which may also result in marked temperature dependence of mechanical properties, such as moduli, in the transition region.

0024-9297/92/2225-6341$03.00/0

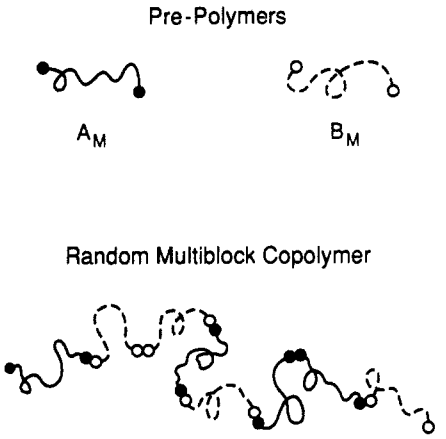

Figure 1. Model random multiblock copolymers considered in the present paper. Each chain consists of Q flexible segments, each of which can be of either type-A (solid) or type-B (dashed). The segments in turn are prepolymers, each composed of M monomers of A or B. The distribution of segments along a chain depends on a parameter λ whose value is dictated by the coupling chemistry as described in section II.

In the present paper we provide a more detailed exposition of these results but in the context of a class of random multiblock copolymer materials formed by random couplings of A_M and B_M prepolymers with (equal) degrees of polymerization $M \sim 10$–100 to build multiblock chains with an overall degree of polymerization $N = MQ$. For large numbers of segments, $Q \gtrsim 10$, we find that such materials should exhibit the same ordering and multicritical phenomena as predicted for random copolymers, but these phenomena should be observable for a much larger class of noncrystalline, flexible A–B monomer pairs, including common pairs such as styrene–butadiene. We are hopeful that due to the unusual temperature sensitivity near the ODT discussed above, such multiblock materials could have novel properties that might lead to important applications.

II. Model and Sequence Distributions

In the present paper we consider an idealized model of a random multiblock copolymer melt, which nevertheless could be closely realized in certain model systems. As depicted in Figure 1, the random multiblock copolymers of interest are constructed from bifunctional, "living" prepolymers of species A and B, A_M and B_M. For simplicity, we take these prepolymers to be built from exactly M monomers of either A or B and choose the monomers to have the same size (the volume of a monomer is taken to be unity), shape, and flexibility (statistical segment length b). In practice, of course, one should relax these assumptions, but for our present purpose this will prove unnecessary. Next, we assume that a coupling agent is available to randomly copolymerize mixtures of the two prepolymers into linear multiblock chains. For simplicity, we take the multiblock copolymers produced to be perfectly monodisperse with a total of Q prepolymers per chain, or $N = QM$ total monomers per chain. In the following discussion, we shall use the term *segment* to refer to individual prepolymer units incorporated in a multiblock chain and the term *block* to refer to a contiguous sequence of prepolymer units of the same type.[14] Hence, a block may consist of just one segment, as in an alternating copolymer, or of any number of segments, as in random copolymers.

For the purpose of describing the monomer sequences that are produced by the coupling reaction we employ the traditional first-order Markov model of random copolymerization.[28] In this model, the reactivity of an unreacted prepolymer toward a growing chain end depends only on the type of free prepolymer and the type of end segment. Hence, a matrix of four bimolecular reaction rate constants, k_{KL} ($\{K, L\}$ = A or B), suffices to specify the chain propagation kinetics. Here, k_{KL} is the rate constant for a reactive (e.g., free radical, cation, or anion) chain end of type L to add a free prepolymer of type K. A further simplifying assumption is that the coupling reaction is carried out in a continuous reactor running under steady-state conditions. The concentration of unreacted prepolymers in the reactor and the average composition of the growing multiblocks can thus be taken to be time-independent, permitting a simple steady-state kinetic analysis of the block sequence distribution. The stochastic process generated under such conditions is said to be a *stationary* first-order Markov process.[29]

Complete specification of the block sequence distribution in the first-order Markov model requires that only *two* parameters be determined. The first is the average copolymer composition, f, which is simply the *average* mole (or volume) fraction of type-A monomers (or segments) that are incorporated into the Q-segment chains. By the steady-state assumption, f can also be interpreted as the probability that a segment at an arbitrary position along a chain is of type A. Clearly, the probability of an arbitrary segment being of type B is $1 - f$. The second quantity that would seem to be necessary to specify the sequence distribution is actually four quantities: a 2×2 matrix of pair probabilities, p_{KL}, giving the conditional probability that a segment of type L (A or B) at some arbitrary location on a chain is immediately followed by a segment of type K (A or B). However, by conservation of probability two of the pair probabilities can be eliminated:

$$p_{BA} = 1 - p_{AA} \tag{2.1}$$

$$p_{AB} = 1 - p_{BB} \tag{2.2}$$

A third relationship among the p_{KL} results from the stationary assumption that f and p_{KL} are independent of location on the chain. Hence

$$f = p_{AA} f + p_{AB}(1 - f) \tag{2.3}$$

From eqs 2.1–2.3 it is clear that only *one* element of the p_{KL} matrix is independent. It proves convenient to choose this one degree of freedom as the linear combination

$$\lambda = p_{AA} + p_{BB} - 1 \tag{2.4}$$

which coincides with the only nontrivial eigenvalue of the p_{KL} matrix (the other eigenvalue is unity).

In the following analysis, we shall treat the copolymer composition f and the parameter λ as independent variables and express all other quantities related to the block sequence distribution in terms of these variables. For example, it follows from eqs 2.2–2.4 that the conditional probabilities p_{AA} and p_{BB} can be written as

$$p_{AA} = f(1 - \lambda) + \lambda \tag{2.5}$$

$$p_{BB} = f(\lambda - 1) + 1 \tag{2.6}$$

Although the calculations in the present paper will be focused on developing the thermodynamic properties of our model multiblock copolymer as a function of f and λ, it is important to keep in mind that these parameters are related to the reaction rate constants k_{KL} previously

discussed. In particular, the first-order Markov model at steady state leads to the expressions[28]

$$f = \frac{r_A f_0^2 + f_0(1-f_0)}{r_A f_0^2 + 2f_0(1-f_0) + r_B(1-f_0)^2} \tag{2.7}$$

$$\lambda = \frac{r_A f_0}{r_A f_0 + 1 - f_0} + \frac{r_B(1-f_0)}{r_B(1-f_0) + f_0} - 1 \tag{2.8}$$

where $r_A \equiv k_{AA}/k_{BA}$ and $r_B \equiv k_{BB}/k_{AB}$ are ratios of rate constants known as *reactivity ratios* and f_0 is the composition (mole or volume fraction of species A) of the prepolymer feed stream to the reactor. Hence, estimates of f and λ can be obtained from tabulated reactivity ratio data and target feed compositions.[28] Alternatively, f and λ can be directly measured by spectroscopic methods, such as NMR.

As will become apparent in the subsequent analysis, λ is a parameter that characterizes the strength of the chemical correlations along a multiblock chain.[25] (A related parameter θ has been employed in earlier theoretical studies[21] of statistical copolymer blends.) From the definition eq 2.4 it is clear that λ can assume values ranging from -1 to $+1$. The value $\lambda = -1$ is achieved only for $p_{AA} = p_{BB} = 0$, implying that every A segment is followed by a B segment and every B segment is followed by an A segment. Hence, the case of $\lambda = -1$ corresponds to an *alternating multiblock copolymer*, in which all chains have the ordered structure $(A_M B_M)_{Q/2}$. It should be emphasized that there is only *one* molecular species present in a copolymer melt with this extreme value of λ. The opposite limit of $\lambda = 1$ is met only when $p_{AA} = p_{BB} = 1$; hence, $p_{AB} = p_{BA} = 0$. This limit corresponds to a situtation where a reactive type-A segment successively adds only more type-A segments, producing an A *homopolymer* with $N = QM$ total monomers. Similarly, a reactive type-B segment would grow a pure B homopolymer of N monomers in the $\lambda = 1$ limit. Thus, the chains in a multiblock melt characterized by $\lambda = 1$ are of two types: a fraction f of the chains are A homopolymers of length N and the remaining chains (fraction $1 - f$) are B homopolymers of length N. A third special case is that of $\lambda = 0$. As will become apparent below, this corresponds to a situation in which the types of segments at adjacent locations on a chain are completely independent of one another (i.e., uncorrelated). From eq 2.4 we see that this condition, known as *ideal random copolymerization*, is met whenever $p_{AA} + p_{BB} = 1$ (or, equivalently, $r_A r_B = 1$). Unlike the limiting cases of $\lambda = -1$ or $+1$, an ideal random multiblock sample consists of chains that differ in overall composition and/or A–B segment sequencing. Indeed, for all $-1 < \lambda < 1$ a multiblock sample is characterized by a continuous distribution of molecular species, each being selected from the ensemble of 2^Q possible arrangements of A and B segments on a chain, subject to the global constraint that the overall sample composition be fixed at f.

The three limiting cases of λ just discussed are depicted in Figure 2. Multiblock samples that are produced under realistic polymerization conditions usually fall somewhere between these limits and are characterized by values of λ not too close to either extreme limit of -1 or $+1$. Cases of $0 < \lambda < 1$ correspond to multiblock samples with a tendency for "blockiness" (i.e., repeated segments of the same type), the extent of which depends on how close λ is to the upper limit. Similarly, cases of $-1 < \lambda < 0$ correspond to multiblocks with a bias toward alternation of A and B segments along the chain. To make these

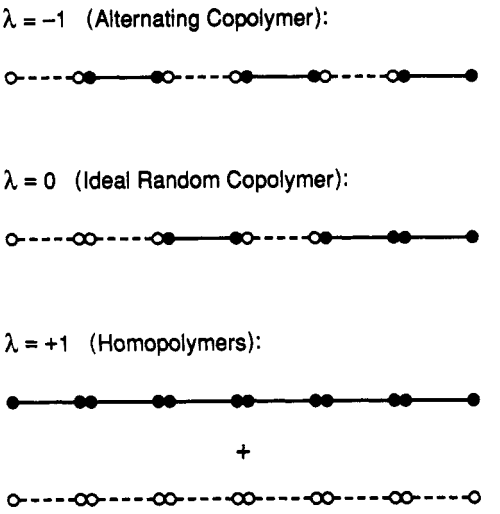

Figure 2. Types of chemical correlations in our model multiblock melt. Samples are characterized by a "blockiness" parameter λ that varies from -1 in the case of a perfectly alternating multiblock copolymer (antiferromagnetic correlations) to $+1$ in the case of a sample consisting of a mixture of pure A and B homopolymers (ferromagnetic correlations). The intermediate case of $\lambda = 0$ corresponds to an ideal random block copolymer in which there are no correlations between the types of segments occupying adjacent positions on a chain.

statements more quantitative and further clarify the physical interpretation of λ, it is helpful to analyze the chemical correlations along the contour of a multiblock. If we label the successive segments of a chain by an index l that runs from 1 to Q and associate with each segment a stochastic Ising variable θ_l, where $\theta_l = 1$ if the segment is type A and $\theta_l = -1$ if the segment is of type B, then the first-order Markov model described above dictates the form of the probability distribution function of the $\{\theta_l\}$. From the previous discussion it should be clear that this joint distribution function depends only on the two parameters f and λ. A convenient way of discussing the features of the distribution is by studying its moments, i.e, correlation functions. As shown in Appendix A, the first two are simply given by

$$\langle \theta_l \rangle_{ave} = 2f - 1 \tag{2.9}$$

$$\langle \theta_l \theta_k \rangle_{ave} - \langle \theta_l \rangle_{ave} \langle \theta_k \rangle_{ave} = 4f(1-f)\lambda^{|l-k|} \tag{2.10}$$

Equation 2.10 confirms our earlier statement that λ describes the strength of the chemical correlations along a multiblock chain. For $\lambda > 0$ these are ferromagnetic correlations, characteristic of "blocky" chains with sequences of repeated A or B segments, while in the case of $\lambda < 0$ the correlations are antiferromagnetic, describing a tendency for A–B alternation.

Finally, we must describe the manner in which the different types of monomers interact in the melt. To crudely account for the repulsive part of the pair interaction potentials, we enforce incompressibility,[6,30] allowing the local composition to fluctuate but not the total monomer density. Furthermore, we account for the difference in the attractive parts of the pair potentials by the conventional[30,31] Flory χ parameter, which describes in units of $k_B T$ (and per monomer) the enthalpy penalty of A–B monomer contacts relative to A–A and B–B contacts. For the purpose of this paper, we consider

systems where χ *increases with decreasing* temperature according to $\chi \sim 1/T$. The formulas derived here apply also to A–B monomer pairs where χ increases with temperature, but the descriptive language (i.e., cooling or heating) must be reversed.

III. Thermodynamic Properties

A. Landau Free Energy Functional. We now turn to consider the phase behavior and thermodynamic properties of the model random block copolymer melt described in the last section. Our approach is to construct a Landau-type density functional theory[15] in which the free energy $F[m]$ is developed as a functional Taylor expansion in a concentration order parameter field $m(\mathbf{x})$. A convenient choice for $m(\mathbf{x})$ is[15,24,25]

$$m(\mathbf{x}) = \langle \langle \phi_A(\mathbf{x}) - f \rangle \rangle_{ave} \tag{3.1}$$

where $\phi_A(\mathbf{x})$ is the *microscopic* volume fraction of type-A monomers at position $\mathbf{x}$, which depends on the instantaneous monomer positions, $\{\mathbf{R}\}$, and the distribution of monomers along the chains, i.e., realization of occupation variables $\{\theta\}$. The inner average in eq 3.1 is an ensemble (thermal) average over $\{\mathbf{R}\}$, and the outer is a quenched average over $\{\theta\}$. An equivalent, but microscopic, expression for $m(\mathbf{x})$ is given in Appendix B, eq B.5.

The field $m(\mathbf{x})$ is useful for the purpose of studying the phase behavior of copolymer melts since it vanishes identically in a single homogenous (liquid) phase but takes nonzero uniform values in coexisting liquid phases. In the case of a mesophase, there exists a set of Fourier coefficients of $m(\mathbf{x})$, denoted $\{m(\mathbf{k})\}$, that are nonvanishing. Hence, by minimizing a suitable free energy functional $F[m]$ with respect to the Fourier coefficients of m, it is possible to distinguish different types of phases and to delineate different regions of the phase diagram.

In Appendix B we present a derivation of the mean-field free energy functional to fourth order in m, enforcing incompressibility of the melt and describing the enthalpy of contacts between dissimilar A and B monomers by the phenomenological parameter χ. The method employed is an extension of that developed by Fredrickson and Leibler[22] and avoids the use of replica averaging techniques.[24,25] We have simplified the expansion coefficients by retaining only leading order terms in the number of segments per chain, i.e., $Q \gg 1$, and only terms up to first order in the strength of the chemical correlations, $|\lambda| \ll 1$. Relative to the free energy of a single homogenous phase ($m = 0$), the free energy functional can be written as

$$F[m] = \frac{1}{2!V}\sum_{\mathbf{k}} m(\mathbf{k})\, m(-\mathbf{k})\, [G_2^{-1}(k^2R_M^2) - 2\chi] - \frac{C_3}{3!C_2^2MV^2}\sum_{\mathbf{k}_1}\sum_{\mathbf{k}_2} m(\mathbf{k}_1)\, m(\mathbf{k}_2)\, m(-\mathbf{k}_1-\mathbf{k}_2) + \frac{N}{4(C_2M\Lambda)^2V^3}\sum_{\mathbf{k}_1}\sum_{\mathbf{k}_2} m(\mathbf{k}_1)\, m(-\mathbf{k}_1)\, m(\mathbf{k}_2)\, m(-\mathbf{k}_2) \times g(k_1^2R_N^2 + k_2^2R_N^2) \tag{3.2}$$

where $g(x)$ is the Debye function (eq B.18) and $G_2(x)$ is a Debye-like function defined by eq B.19. We have also made the following definitions:

$$\Lambda \equiv \frac{1+\lambda}{1-\lambda} \tag{3.3}$$

$$C_2 \equiv f(1-f), \quad C_3 \equiv 1-2f \tag{3.4}$$

The unperturbed mean-squared radii of gyration of a segment and a chain are given, respectively, by

$$R_M^2 = Mb^2/6$$

$$R_N^2 = Nb^2/6 = Q\,R_M^2 \tag{3.5}$$

In the cubic and quartic terms of eq 3.2 we have also coarse-grained the Landau coefficients on the scale of a segment radius of gyration, R_M, by taking $k_iR_M \ll 1$, where k_i is the magnitude of a wavevector in the sums. Finally, we note that the overall volume of the sample is denoted V and the Fourier coefficients $m(\mathbf{k})$ are defined in terms of $m(\mathbf{x})$ by eq B.15.

Before discussing the consequences of eq 3.2, we should point out that the equation is consistent with previous expressions derived for random (statistical) copolymers. In particular, if one sets $M = 1$ in the equation, an expression results that was employed by Fredrickson and Milner[25] in their study of random copolymer melts; if one further takes $N \to \infty$ and $\lambda = 0$, the free energy functional of Shakhnovich and Gutin[24] is recovered. Finally, the limit of $M = 1$, $\lambda = 0$, and $k_iR_N \ll 1$ was previously obtained by Fredrickson and Leibler.[22] As was discussed in ref 22, this long-wavelength limit is consistent with a "pseudo-binary approximation" in which the continuous distribution of chain compositions is replaced by a sum of two δ functions with the same variance as the original distribution. Flory-Huggins theory for the pseudo-binary system, when expanded in powers of m, leads to a free energy expression with the same scaling behavior as the long-wavelength limit ($k_iR_N \ll 1$) of eq 3.2.

B. Spinodal Conditions. The stability limit of the homogenous liquid phase of a random multiblock copolymer melt is determined by the condition

$$\min_k [G_2^{-1}(k^2R_M^2) - 2\chi] = 0 \tag{3.6}$$

For the situations of primary interest here the minimum values of k, denoted k^*, will satisfy $k^*R_M \ll 1$; hence, it is sufficient to expand $G_2^{-1}(x)$ to $O(x^2)$, leading to

$$\min_k \left[1 - 2C_2M\Lambda\chi + \frac{1+4\lambda+\lambda^2}{3(1+\lambda)(1-\lambda)}(kR_M)^2 + \frac{(kR_M)^4}{36\Lambda^2} \right] = 0 \tag{3.7}$$

While the $O(k^4)$ coefficient is always positive, the coefficient of the $O(k^2)$ term is only positive if

$$\lambda > \lambda_L \equiv -2 + \sqrt{3} \approx -0.268 \tag{3.8}$$

In such cases of $\lambda > \lambda_L$, the expression in eq 3.7 is minimized by $k^* = 0$ and the spinodal condition reduces to ($\chi = \chi_s$)

$$\chi_sM = \frac{1}{2C_2\Lambda} = \frac{1-\lambda}{2f(1-f)(1+\lambda)} \tag{3.9}$$

This expression is valid provided that $|\lambda|^Q \ll 1$. A uniformly accurate expression for $0 \le \lambda \le 1$, however, comes from restoring the subdominant terms in Q to eq B.19:[25]

$$\chi_sM = \frac{Q(1-\lambda)^2}{2f(1-f)\{Q(1-\lambda)^2 + 2\lambda[Q(1-\lambda) + \lambda^Q - 1]\}} \tag{3.10}$$

Equations 3.9 and 3.10 are indistinguishable for $Q \gg 1$, except for values of λ that are within Q^{-1} of +1. Precisely at $\lambda = 1$, the homopolymer limit (cf. Figure 2), eq 3.10 recovers the exact Flory–Huggins spinodal[30] $\chi_s = 1/[2f(1-f)N]$, while eq 3.9 incorrectly gives $\chi_s = 0$. In the following

analysis, however, we shall use the simpler eq 3.9 unless explicitly stated otherwise.

Equation 3.9 (or 3.10) for $\lambda_L < \lambda < 1$ describes the limit of stability of a single homogenous copolymer phase to phase separation into *two* coexisting liquid phases. (Note that the quartic coefficient in eq 3.2 is positive; hence, we expect that $F[m]$ will have at most two low-lying minima for χ very near χ_s.) At $\lambda = 1$, this behavior is easily understood as the partitioning of A and B homopolymers. For the more general $\lambda_L < \lambda < 1$ a similar interpretation is possible.[25] The average composition (volume fraction of A) of a *single* multiblock chain can be written as

$$c = \frac{1}{2Q}\sum_{l}(1 + \theta_l) \tag{3.11}$$

where $\langle c \rangle_{ave} = f$. The probability distribution function of c, $P(c)$, in the case of $\lambda = 1$ is the simple bimodal distribution

$$P(c) = f\delta_{c,1} + (1-f)\delta_{c,0} \tag{3.12}$$

and it is the partitioning of the different molecules (chains) belonging to the two parts of the distribution that we interpret as phase separation. For $\lambda = 0$, however, the θ_l variables along a chain are independent, so the central limit theorem implies that $P(c)$ is Gaussian for large Q, with mean f and variance $\langle (\delta c)^2 \rangle_{ave} = f(1-f)/Q$. Again the phase separation can be interpreted as a partitioning (by chain) of $P(c)$, but division of the singly-peaked Gaussian distribution in the case of $\lambda = 0$ produces two phases that differ at most by $\langle (\delta c)^2 \rangle_{ave}^{1/2} = [f(1-f)/Q]^{1/2}$ in composition. We shall see later that eq 3.2 is indeed consistent with this prediction. For more general values of $\lambda_L < \lambda < 1$, but $|\lambda|^Q \ll 1$, the distribution $P(c)$ remains singly peaked and the above argument can be extended to conclude that the two coexisting phases differ at most in composition by $\langle (\delta c)^2 \rangle_{ave}^{1/2} = [f(1-f)\Lambda/Q]^{1/2}$.

It is interesting to contrast these predictions of liquid–liquid phase separation in a *pure* random copolymer sample of mean composition f and "blockiness" λ with earlier predictions[21] of phase separation in blends of random copolymers that differ in composition and/or sequence distribution. In these treatments of copolymer blends, for which the overall chain composition distribution $P(c)$ is doubly peaked, each pure random copolymer (with a singly peaked chain composition distribution) is imagined to be a single component. While such lumping is permissible for the situations considered by the authors of ref 21, it would not be capable of describing the phase-separation behavior discussed above. Indeed, we rely on the finite width of the singly-peaked $P(c)$ for a pure random copolymer melt to give the predicted liquid–liquid separation.

For cases of $\lambda < \lambda_L$ (strong tendency for alternation of segments), the $O(k^2)$ coefficient in eq 3.7 changes sign, and $k^* \neq 0$. On minimization, one obtains

$$(k^*R_M)^2 = \frac{6(1+\lambda)(\lambda + 2 + \sqrt{3})(\lambda_L - \lambda)}{(1-\lambda)^3} \tag{3.13}$$

which is valid for λ in the close vicinity of λ_L. For smaller values of λ it is not permissible to expand $G_2^{-1}(x)$; k^* must be determined numerically by minimization of eq 3.6. As shown in Figure 3, $(k^*R_M)^2$ increases monotonically from zero as λ is reduced below λ_L. In the limit of a perfectly alternating multiblock melt, $\lambda = -1$, $(k^*R_M)^2 \approx 3.2$ which is consistent with earlier theoretical work.[6-11] An interesting feature of eq 3.13 (and Figure 3) is the independence

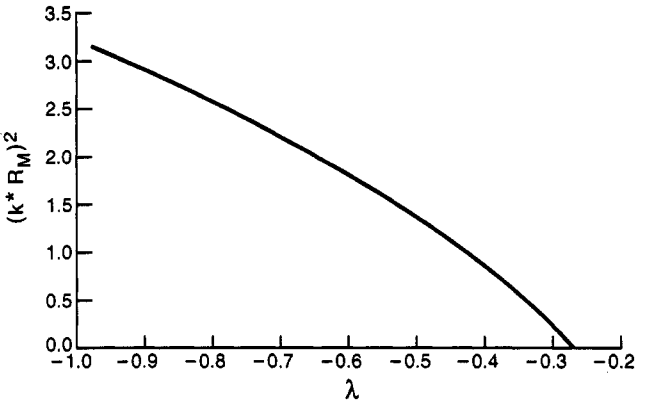

Figure 3. Dependence of the wavevector k^*, which characterizes the microphase period at the spinodal for $\lambda < \lambda_L$, on the parameter λ. In the close vicinity of λ_L, k^* is given by eq 3.13, but it is obtained more generally by numerical minimization of eq 3.6.

of k^* on f, unlike monodisperse diblock or triblock copolymers where k^* exhibits a reasonably strong dependence on composition.

Equation 3.13 gives the wavevector k^* that characterizes the most unstable concentration wave on cooling a multiblock sample with $\lambda \leq \lambda_L$ to the point where a *microphase separation* first occurs (i.e., the ODT).[15] This wavevector also describes the location of the peak in the structure factor for a homogenous multiblock melt (see the Discussion section). Substitution of eq 3.13 into eq 3.7 leads to an equation for the $\lambda \leq \lambda_L$ *microphase spinodal line* ($\chi = \chi_{sm}$):

$$\chi_{sm}M = \frac{(1-\lambda)^4 - (\lambda + 2 + \sqrt{3})^2(\lambda_L - \lambda)^2}{2f(1-f)(1-\lambda)^3(1+\lambda)} \tag{3.14}$$

This microphase spinodal line smoothly joins the liquid–liquid spinodal line eq 3.9 at the point

$$\lambda_L = -2 + \sqrt{3} \approx -0.268$$

$$\chi_L M = \frac{1-\lambda_L}{2f(1-f)(1+\lambda_L)} \approx \frac{1.73}{2f(1-f)} \tag{3.15}$$

For the special case of $f = f_L = 1/2$, this point is a special type of multicritical point[32,33] known as an *isotropic Lifshitz point*, being at the confluence of $k^* = 0$ and $k^* \neq 0$ critical lines. For cases of asymmetric copolymers, $f \neq 1/2$, these lines are spinodal lines and the Lifshitz points given by eq 3.15 are preempted by first-order transitions, as will be described below. In Figure 4 we plot the two branches of the spinodal lines given by eqs 3.9 and 3.14 as functions of λ. On crossing the solid curve to the right of $\lambda_L = -0.268$ (e.g., by lowering temperature and hence increasing χ), a homogenous melt becomes unstable to separation into two liquid phases. On crossing the solid curve to the left of λ_L, a homogenous melt becomes unstable to a microphase characterized by wavevectors of magnitude k^* given in eq 3.13. As is typical of mean-field analyses of Lifshitz points, k^* vanishes continuously according to $(\lambda_L - \lambda)^{1/2}$ as the Lifshitz point is approached from the left. Hence, in the close vicinity of λ_L, the microphase period $2\pi/k^*$ can greatly exceed either the segment size R_M or the overall chain size R_N. The spatially varying composition patterns in this regime are built up by distributing *entire chains* according to their composition, with chains characterized by $c > f$ forming the A-rich microdomains and chains with $c < f$ forming the B-rich domains. Finally, we should note that since eq 3.14 is

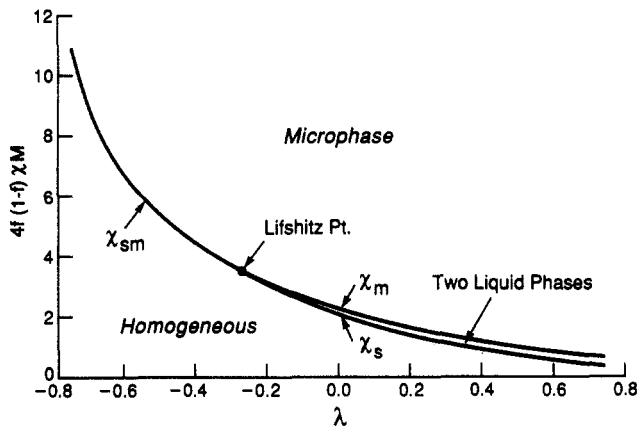

Figure 4. Spinodal lines for a random multiblock melt of variable λ. On cooling a melt with $\lambda > \lambda_L \approx -0.268$, the first instability is to phase separation into two homogenous liquid phases ($\chi = \chi_h$). On further cooling to $\chi = \chi_m$, the two liquid phases become unstable to the formation of a microphase. In contrast, a melt with $\lambda < \lambda_L$ first becomes absolutely unstable to the formation of microphases ($\chi = \chi_{sm}$). At the critical composition of $f = 1/2$, the point (λ_L,χ_L) is a multicritical point known as an isotropic Lifshitz point.

based on the expansion 3.7, it is not accurate for values of λ that are significantly less than λ_L.

C. Stability of Homogenous Phases. In order to fill in the remainder of the random multiblock phase diagram, it is necessary to use eq 3.2 to calculate the free energy of different proposed homogenous or inhomogenous phases. We begin by considering the free energy of multiple homogenous phases for $\lambda > \lambda_L$. In such cases the relevant Fourier coefficients are $m(\mathbf{k})$ with k^{-1} comparable to the macroscopic size of a phase. (Note, however, that $m(\mathbf{k}=0)$ is strictly zero.) Under such circumstances we can set k_iR_M and k_iR_N to zero in eq 3.2, yielding a purely local free energy density

$$F/V = (\chi_s - \chi)m^2 - \frac{C_3}{3!C_2^{\,2}M}m^3 + \frac{N}{4(C_2M\Lambda)^2}m^4 \qquad (3.16)$$

where m is the value of $m(\mathbf{x})$ in a homogenous phase of macroscopic extent and χ_s is given by eq 3.9. It will prove convenient to reexpress eq 3.16 by introducing a new free energy density, F_H, defined by

$$F_H = 2M(F/V) = 2M(\chi_s - \chi)m^2 - \alpha m^3 + \beta m^4 \qquad (3.17)$$

with

$$\alpha \equiv \frac{C_3}{3C_2^{\,2}} = \frac{1-2f}{3f^2(1-f)^2} \qquad (3.18)$$

$$\beta = \frac{Q}{2C_2^{\,2}\Lambda^2} = \frac{Q(1-\lambda)^2}{2f^2(1-f)^2(1+\lambda)^2} \qquad (3.19)$$

Equation 3.17 can be used to study the liquid–liquid phase separation that occurs for $\lambda > \lambda_L$. Minimizing eq 3.17 yields (nonzero root of lowest free energy)-$m = \bar{m}$

$$\bar{m} = 3\alpha(1+\gamma)/(8\beta) \qquad (3.20)$$

with

$$\gamma = [1 - 64\beta(\chi_s - \chi)M/(9\alpha^2)]^{1/2} \qquad (3.21)$$

The homogenous molten phase first becomes metastable (or unstable for $f = 1/2$) with respect to two liquid phases

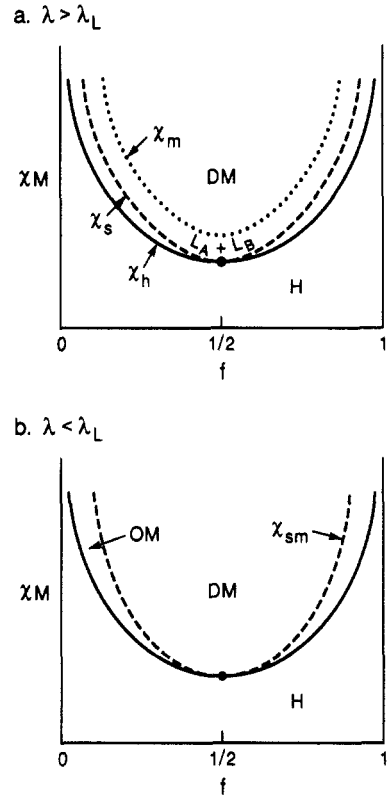

Figure 5. (a) Schematic phase diagram in the coodinates χM and f for the case of $\lambda > \lambda_L$. The notations H, $L_A + L_B$, and DM denote, respectively, regions of stability for the homogenous phase, coexistence of two liquid phases, and disordered microphases (i.e., no long-range order). (b) Schematic phase diagram in the coodinates χM and f for the case of $\lambda < \lambda_L$. The notation OM denotes regions where long-range ordered microphases (e.g., hexagonal, bcc, etc.) are expected to be stable.

very near the point at which $F_H(\bar{m}) = 0$, which leads to the condition ($\chi = \chi_h$)

$$\chi_h M = \chi_s M - \alpha^2/(8\beta) = \chi_s M - \frac{(1-2f)^2(1+\lambda)^2}{36f^2(1-f)^2(1-\lambda)^2Q} \qquad (3.22)$$

This equation describes the binodal curve for liquid–liquid phase separation, which, due to the factor Q^{-1}, lies very close to the spinodal. Because the cubic term in eq 3.17 vanishes for compositionally symmetric melts, $f = 1/2$ is evidently a critical point at which the phase separation is second order, while the transition is first order at all other points along the binodal. For $f \neq 1/2$ droplets of composition $f + \bar{m}$ are expected to nucleate in the homogenous copolymer melt on raising χ above χ_h. As χ is further raised above χ_h (e.g., by lowering T), the compositions of the two coexisting phases can be easily obtained from eq 3.17 by equating the exchange chemical potentials, $\mu = \partial F_H/\partial m$, and osmotic pressures, $\Pi = F_H - \mu m$, of the two phases. However, an order of magnitude estimate of the composition difference between phases is given by $\bar{m}$, the minimum of F_H, which from eq 3.20 is characteristically $(1-2f)\Lambda^2/(3Q)$ at the first-order transition and increases to be of order $[(\chi/\chi_s - 1)f(1-f)\Lambda/Q]^{1/2}$ above the transition. This latter result is in accord with the pseudo-binary approximation,[22] discussed in the previous section.

In Figure 5 we show a schematic drawing of the binodal and spinodal curves in the χM verses f plane for $\lambda > \lambda_L$. It is *important* to note that tie lines cannot be drawn in this plane, since f is a parameter that characterizes the distribution of molecular species and does not reflect the local composition of coexisting phases. The tie lines can

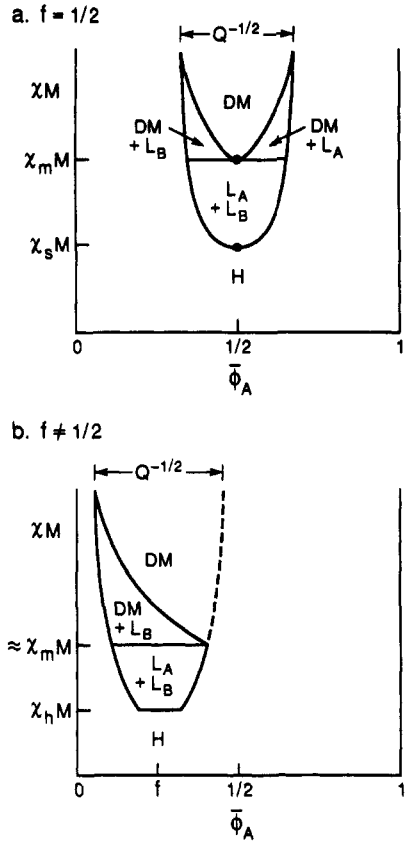

Figure 6. (a) Schematic phase diagram in the coodinates χM and $\bar{\phi}_A$ for the case of $\lambda > \lambda_L$ and $f = 1/2$, where $\bar{\phi}_A$ is the local volume fraction of type A monomers. The notations for the phases are the same as in Figure 5, but the present representation allows for the construction of tie lines parallel to the $\bar{\phi}_A$ axis to determine the compositions of coexisting phases. On phase separation into two liquid phases differing in composition by $O(Q^{-1/2})$, a symmetric copolymer melt freezes in a eutectic-like fashion into a disordered mesophase. (b) Schematic phase diagram in the coordinates χM and $\bar{\phi}_A$ for the case of $\lambda > \lambda_L$ and $f \neq 1/2$. After a first-order separation into two liquid phases, the liquid phase with composition closest to $1/2$ freezes into a disordered mesophase, whose composition changes until the freezing is complete and the other liquid phase is consumed. The usual lever rule applies in this plane, and tie lines can be drawn in both two-phase regions.

instead by represented in a χM verses $\bar{\phi}_A$ plane, where $\bar{\phi}_A \equiv \bar{m} + f$ and f are treated as being independent. Schematic examples of such diagrams are shown in Figure 6 for critical ($f = 1/2$) and off-critical ($f \neq 1/2$) compositions.

D. Microphase Free Energy and Stability. We now turn to consider the free energy of inhomogenous structures (i.e., microphases) and the possibility that the coexisting liquid phases will lose stability to such microphases on further cooling. For large enough values of χ we expect that microphases would be preferred over homogenous phases because the former allow for complete local segregation of A and B monomers, while the latter retain practically all of the A–B contacts of the single mixed phase. For simplicity and for consistency with the mean-field theory of diblock copolymers developed by Leibler,[15] we adopt a single-harmonic approximation for the microphase structures. In particular, we choose the following representation for $m(\mathbf{x})$:

$$m(\mathbf{x}) = \frac{2}{n^{1/2}}\psi_n \sum_{i=1}^{n} \cos(\mathbf{K}_i \cdot \mathbf{x}) \tag{3.23}$$

where the set of reciprocal lattice vectors $\{\mathbf{K}_i\}$ ($i = 1, ..., n$) have equal magnitudes $|\mathbf{K}_i| = k$ and are chosen to describe lamellae ($n = 1$), cylinders ($n = 3$), and bcc spheres ($n = 6$) in the usual way.[11,15] The lattice vector magnitude k and pattern amplitude ψ_n will be treated as variational parameters and subsequently eliminated. Besides these long-range-ordered microphase structures, we have also considered *disordered*, random wave structures of the form[24,25]

$$m(\mathbf{x}) = \frac{2\psi_\infty}{I^{1/2}} \sum_{i=1}^{I} \cos(k\hat{\mathbf{n}}_i \cdot \mathbf{x} + \phi_i) \tag{3.24}$$

where the unit vectors $\hat{\mathbf{n}}_i$ are selected uniformly on the unit sphere, the ϕ_i are random phases, and I is a large positive integer (that will later taken to infinity). Such constructs have been used to model time-dependent and stationary patterns observed in spinodal decomposition experiments and microemulsions. Here we use eq 3.24 as an ansatz for an *equilibrium* structure in random multiblock melts.

Substitution of these expressions for $m(\mathbf{x})$ into eq 3.2 yields a free-energy density, $F_n = F[m]M/V$, given by

$$F_n = \{2M(\chi_s - \chi) + 2\chi_s M[Ek^2R_M^2 + (k^2R_M^2)^2/(36\Lambda^2)]\}\psi_n^2 - A_n\psi_n^3 + B\psi_n^4 \tag{3.25}$$

Here we have expanded $G_2^{-1}(x)$ to $O(x^2)$ and made the definitions

$$E \equiv \frac{(\lambda + 2 + \sqrt{3})(\lambda - \lambda_L)}{3(1-\lambda)(1+\lambda)} \tag{3.26}$$

$$B \equiv \frac{Q(1-\lambda)^2 g(2k^2R_N^2)}{f^2(1-f)^2(1+\lambda)^2} \tag{3.27}$$

In the present calculation to leading order in Q^{-1}, only the cubic coefficients depend on the type of structure, i.e., on n. We obtain for lamellae and the random wave structure

$$A_1 = A_\infty = 0 \tag{3.28}$$

while for cylinders (hexagonal phase)

$$A_3 = \frac{2C_3}{3\sqrt{3}C_2^2} \tag{3.29}$$

and for spheres (bcc phase)

$$A_6 = \frac{4C_3}{3\sqrt{6}C_2^2} \tag{3.30}$$

We begin our analysis of the microphases by considering the symmetric case of $f = 1/2$ and $\lambda > \lambda_L$. In this instance $A_n = 0$ for all structures (note $C_3 = 0$), leaving the free-energy expression 3.25 degenerate to the type of structure. It turns out that this degeneracy is weakly broken by contributions to the quartic coefficient in the free energy that are smaller than the leading term by a factor of Q^{-1}. However, since any resulting differences in free energies of the various structures are necessarily small, we expect that in practice *disordered microphases* lacking long-range order will be formed on cooling from the homogenous melt. Since we have little insight into the detailed topology of such microphases, eq 3.24 is employed as a sensible and computationally tractable structural ansatz.

Proceeding with the evaluation of the free energy, eq 3.25 can be minimized with respect to ψ_n (for the case of $A_n = 0$) to obtain

$$F_n = -\frac{[1 - \chi/\chi_s + Ek^2R_M^2]^2}{4Qg(2k^2R_N^2)} \tag{3.31}$$

In this expression we require $\chi/\chi_s > 1 + Ek^2R_M^2$ in order that $|\psi_n| > 0$ and we have dropped the k^4 term in eq 3.25 for the present case of $\lambda > \lambda_L$. Next, we introduce the variables

$$\kappa \equiv (\chi/\chi_s - 1)Q/E$$

$$x \equiv k^2R_N^2 \tag{3.32}$$

and rewrite eq 3.31 as

$$F_n = -\frac{E^2}{4Q^3}\frac{(\kappa - x)^2}{g(2x)} \tag{3.33}$$

The remaining task is to minimize this expression with respect to x (i.e., k). For $\kappa < 3$, eq 3.33 is minimized by $x = 0$, in which case the equation reduces to the free energy of coexisting *homogenous* phases:

$$F_n = -(\kappa^2E^2)/(4Q^3) = F_H/2 \tag{3.34}$$

Thus, at the critical composition the coexisting liquid phases are stable for $0 < \kappa < 3$, or equivalently for χM, satisfying

$$\chi_sM < \chi M < \chi_sM + \frac{(\lambda + 2 + \sqrt{3})(\lambda - \lambda_L)}{2Qf(1-f)(1+\lambda)^2} \tag{3.35}$$

When κ is increased slightly above the critical value of 3, the right-hand side of eq 3.33 is minimized by a nonzero value of x ($x = x_0$):

$$x_0 = \frac{1}{2}(\kappa - 3) + O[(\kappa - 3)^2] \tag{3.36}$$

The corresponding microphase free energy, given by

$$F_n = -\frac{\kappa^2E^2}{4Q^3}\left[1 + \frac{1}{18}(\kappa - 3)^2 + ...\right] \tag{3.37}$$

is then lower than the homogenous free energy given by eq 3.34. Thus, a continuous (second-order) phase transition from two coexisting liquid phases to a disordered microphase occurs at $\kappa = 3(\chi = \chi_m)$:

$$\chi_mM = \chi_sM + \frac{(\lambda + 2 + \sqrt{3})(\lambda - \lambda_L)}{2Qf(1-f)(1+\lambda)^2} \tag{3.38}$$

This line is shown in the χM verses λ plane in Figure 4 and in the χM verses f plane in Figure 5. As is expressed most clearly in the χM verses $\bar{\phi}_A$ plane in Figure 6, two liquid phases and one mesophase coexist at χ_mM. The composition $f = 1/2$ is analogous to a eutectic in binary alloys. The wavevector of the microphase should vary in the transition region according to ($\chi \geq \chi_m$) (cf. eq 3.36)

$$(k_0R_M)^2 = \frac{3f(1-f)(1+\lambda)^2(\chi M - \chi_mM)}{(\lambda + 2 + \sqrt{3})(\lambda - \lambda_L)} \tag{3.39}$$

Similar predictions for statistical copolymers ($M = 1$) have recently been made,[24-27] although the predictions here are universal (do not involve additional phenomenological parameters) because the k^2 coefficients in the free energy are dominated by the nonlocal configurational entropy of a segment and not by the nonlocality of the interactions (i.e., χ).[25]

The last result, eq 3.39, could have important implications for the design of new materials with high-temperature sensitivity. Model diblock and triblock copolymers are known to form microphases characterized by wavevectors k_0 that are only weakly temperature dependent at the ODT.[15,17] Moreover, in such systems k_0 has been observed[16] to *decrease* slightly on cooling (increasing χ), due to copolymer polarization (stretching) caused by the inhomogenous chemical environment surrounding each chain. In contrast, eq 3.39 suggests that for the case of random multiblocks k_0 should *increase* on cooling according to $k_0 \sim (\chi - \chi_m)^{1/2}$. This difference in the behaviors of the two types of block copolymer systems arises from the broad distribution of block sequence lengths in the random system. Near the microphase transition at χ_m, it is the longest contiguous sequences of A or B blocks that are the most incompatible and hence participate to the largest extent in establishing k_0. As the temperature is lowered, shorter A and B sequences begin to "fill in" the microphases, producing a decrease in the period—hence an increase in k_0. In contrast, monodisperse diblock or triblock copolymers have only one block size and thus do not have the luxury of selecting different portions of the sequence length distribution at each temperature. Small-angle neutron or X-ray scattering experiments on labeled random multiblock or statistical copolymers would seem to provide an ideal means for testing eq 3.39.

As a next step, we turn to consider microphase formation at off-critical compositions, $f \neq 1/2$, and $\lambda > \lambda_L$. Naively, the presence of the cubic term in eq 3.25 would be expected to lead to a first-order transition into the bcc structure on sufficient cooling of the coexisting liquid phases. (The bcc phase would be favored over the hexagonal phase since $A_6 > A_3$). However, on minimizing eq 3.25 with respect to ψ_n, it can easily be shown that the cubic term gives a negligible contribution to the free energy when the following condition is met:

$$\chi M - \chi_sM \gg \frac{(1-2f)^2(1+\lambda)^2}{Qf^2(1-f)^2(1-\lambda)^2} \tag{3.40}$$

This difference is very small, of order Q^{-1}, unless f is within Q^{-1} of 0 or 1, or λ is within Q^{-1} of 1. Thus, once χM reaches such values, the choice of microphase structure is determined only by the quartic coefficients, which to leading order in Q^{-1} are independent of structure. We recall, however, that for $f = 1/2$ (eq 3.38) microphases are only possible if $\chi M - \chi_sM \gtrsim Q^{-1}$. One can show from eq 3.25 that this is also the case for arbitrary f (but not too close to 0 or 1). Thus, we expect that for the values of χN sufficient to produce microphase ordering, the contribution of the cubic terms to the free energy is greatly diminished. It follows that to a good approximation for large Q (and not too asymmetric copolymers) the free energy should again be degenerate to the type of structure.

We conclude, therefore, that the microphase ordering transition for $f \neq 1/2$ should occur in the vicinty of χ_mM given by eq 3.38, but the precise nature of the transition and the type of microphase formed are unclear. To clarify these issues would require restoring some of the subdominant contributions to the quartic coefficient B and an analysis beyond the scope of the present paper. However, because of the presence of small, but finite cubic terms in eq 3.25, the ordering transition for $f \neq 1/2$ is probably weakly first-order. Moreover, the approximate degeneracy of the free energy to structure leads one to expect that *disordered microphases* will also be observed for compositionally asymmetric random multiblock melts.

We summarize our predictions for $\lambda > \lambda_L$ by the schematic phase diagrams in Figures 5 and 6. When a random multiblock copolymer melt is cooled, the system first phase separates into two liquid phases at the binodal $\chi_b M$ given by eq 3.22. For $f = {}^1/_2$ the separation is continuous; otherwise, it is first-order. On further cooling by an amount (χM units) that is $O(Q^{-1})$, the two liquid phases undergo a transformation to a disordered mesophase. For $f = {}^1/_2$ this transformation occurs in a eutectic-like fashion (Figure 6a) at $\chi_m M$ given by eq 3.38, with the two liquid phases being consumed at equal rates. For $f \neq {}^1/_2$, the liquid phase with the more symmetric composition freezes into a disordered microphase in the vicinity of $\chi_m M$ (Figure 6b). As the cooling continues, the composition ϕ_A of the microphase approaches f, at which the freezing is complete. Unlike conventional freezing of simple liquids, however, highly disordered solid phases are produced and the lattice constant changes markedly with temperature according to eq 3.39.

Finally, we turn to consider the situation where $\lambda < \lambda_L$. From our analysis of the spinodal it is clear that the formation of microphases is already favorable at $\chi M = \chi_{sm} M$, given by eq 3.14 for λ near λ_L. Hence, we need not be concerned with multiple homogenous phases but instead consider the microphase free-energy expression 3.25 for cases of $\lambda < \lambda_L$. Again, we begin by treating the case of $f = {}^1/_2$ and then generalize our results to asymmetric compositions. At the critical composition, $A_n = 0$, so eq 3.25 becomes degenerate to the type of structure as before. However, for the present case of $\lambda < \lambda_L$, the coefficient E is negative, requiring that we retain the $O(k^4)$ quadratic term in the free energy. On minimizing the resulting free-energy expression with respect to ψ_n (assuming $\chi \geq \chi_{sm}$), one obtains

$$F_n = -\frac{[1 - \chi/\chi_s - |E|k^2R_M^2 + (k^2R_M^2)^2/(36\Lambda^2)]^2}{4Qg(2k^2R_N^2)} \quad (3.41)$$

Except for λ very close to λ_L, the wavevector k that minimizes eq 3.41 will satisfy $kR_N \gtrsim 1$. In such cases, it is permissible to replace $g(2k^2R_N^2)$ by $1/(k^2R_N^2)$ for the purpose of carrying out the minimization. We find for the optimal wavevector of the microphase ($k = k_0$) the result

$$(k_0R_M)^2 = (k^*R_M)^2 + \frac{3f(1-f)(1+\lambda)^2(\chi M - \chi_{sm}M)}{(\lambda + 2 + \sqrt{3})(\lambda_L - \lambda)} \quad (3.42)$$

where k^* is given by eq 3.13 and we have assumed that $0 < \chi M - \chi_{sm} M \ll 1$. Thus, at the microphase transition threshold (ODT) $\chi = \chi_{sm}$, the wavevector k_0 characterizing the microdomain period $2\pi/k_0$ is precisely equal to k^*. Equation 3.42 indicates that the wavevector k_0 increases as χ is raised above χ_{sm} with the same temperature dependence as was found for $\lambda > \lambda_L$. Indeed, the crossover between eqs 3.39 and 3.42 is smooth for large χM.

The free-energy expression 3.41, when evaluated with $k = k_0$, changes sign at χ_{sm}, and the microphase amplitude ψ_n grows continuously from zero at that threshold. Hence, the ODT at the critical composition is found to be second-order within the present mean-field theory. Again, due to the energetic equivalence of all structures for large Q, we anticipate the formation of disordered microphases lacking long-range compositional order.

The case of asymmetric copolymers with a tendency for alternation ($\lambda < \lambda_L$) can be analyzed in a similar fashion. Due to the presence of the cubic terms in eq 3.25 for $f \neq {}^1/_2$, the ODT will correspond to a first-order phase transition, with the bcc phase being the lowest free-energy structure. The transition will occur at a value of χM that precedes the microphase spinodal $\chi_{sm} M$ by a small distance of order $[(1 - 2f)\Lambda/C_2]^2/Q$. However, on further cooling an asymmetric copolymer melt, we know from our previous discussion that the cubic terms in eq 3.25 become irrelevant to the phase behavior at a comparable distance above $\chi_{sm} M$, i.e., for $\chi M - \chi_{sm} M \gtrsim [(1 - 2f)\Lambda/C_2]^2/Q$. At such values of χ the free energy is degenerate to leading order in Q^{-1} and we again expect disordered microphases. Thus, ordered microphases are to be expected within a narrow range of characteristic width (in χM) $[(1 - 2f)\Lambda/C_2]^2/Q$ about the ODT, while disordered inhomogenous phases should be more prevalent at larger χN. Our free-energy functional, however, is not capable of predicting the loss of stability of the bcc phase to the hexagonal phase or to the random wave structure. Higher order (in Q^{-1}) contributions to the quartic coefficient are required to describe the bcc to hexagonal transition (still lying within Q^{-1} of the ODT), and these would also break the degeneracy of the random wave and long-range ordered structures. Nevertheless, we expect that for large Q the energy differences among the various phases will be sufficiently small that copolymer melts with $f \neq {}^1/_2$ and $\lambda < \lambda_L$ will freeze irreproducibly into a myriad of disordered mesophases. The qualitative features of this postulated phase behavior are shown in Figure 5b.

IV. Discussion

In the present paper we have made a number of predictions for the phase behavior and thermodynamic properties of a restricted class of random multiblock copolymers. An obvious method of testing some of these predictions would be to perform SANS or SAXS experiments on multiblock melts that have been suitably labeled to provide contrast between the two types of segments. Ideally, one would like to have access to both the homogenous phase and the microphases by varying the temperature. Since a large range of χ can generally not be achieved for the restricted range of temperatures to which most systems can be subjected, this necessitates preparing a sample that is close to the threshold for liquid–liquid separation or the ODT. In practice, since all the phase boundaries for long chains are close to the spinodal χ_s, the system should be constructed to allow χ to be varied on either side of χ_s given by eq 3.9. For example, if one were preparing a styrene–diene multiblock with symmetric composition ($f = {}^1/_2$) and by means of coupling chemistry that approximated conditions of ideal copolymerization ($\lambda = 0$), then eq 3.9 reduces to $\chi_s \approx 2/M$. Since χ values for such pairs are of order 0.1 in a workable temperature range, one should try to synthesize prepolymers with degree of polymerization 20.

Having prepared a suitable sample, the next step would be to examine the scattered intensity in the homogenous phase of the copolymer melt. Within the context of the present mean-field theory, the scattered intensity in the homogenous phase is proportional to the reciprocal of the quadratic coefficient in eq 3.2. The relevant structure factor is thus

$$S(k) = 1/[G_2^{-1}(k^2R_M^2) - 2\chi] \quad (4.1)$$

where the function $G_2(x)$ is defined in eq B.19. The k dependence and temperature dependence of the scattered intensity could be tested against eq 4.1. Alternatively, for a sample where the coupling chemistry is poorly understood but the composition f is known, fits of scattering data to eq 4.1 could be used to extract a value of λ and thus provide a measure of the block sequence distribution.

Multiblock samples that are characterized by $\lambda > \lambda_L \approx -0.268$ will, according to eq 4.1, have maximum scattered intensity at $k = 0$ in the homogenous phase. On cooling through the liquid–liquid boundary at $\chi = \chi_h$, there will probably be little change in the scattering, since the composition difference between the two phases is only of order $Q^{-1/2}$—providing little contrast. On further cooling through χ_m given by eq 3.38, however, a peak in the scattering intensity at $k = k_0$ should emerge at small wavevectors. This peak position should move to *larger* values with increasing χ (decreasing T) according to eq 3.39.

In contrast, homogenous samples characterized by $\lambda < \lambda_L$ will show a peak in their scattered intensity at a wavevector k^* given by eq 3.13. On cooling within the homogenous phase, this peak position should show only the weak temperature dependence seen in monodisperse diblock copolymers[17] until the ODT is reached. At that point, the peak is expected to move to higher values of k in the manner predicted by eq 3.42.

The unique temperature dependence of the peak position, as was described in detail in the previous section, arises from the broad distribution of block lengths present in random systems and is not (e.g.) a feature of perfectly alternating multiblock copolymers ($\lambda = -1$). Since the mechanical and optical properties of microphase-separated block copolymers are strong functions of the microdomain period, we expect these properties to also exhibit marked temperature sensitivity for the case of the random multiblock materials. Thus, we are left with the interesting conclusion that multiblock properties might actually be enhanced by purposefully introducing disorder in the form of block polydispersity. It would seem that thermoplastic elastomers, polyurethanes, or other polymeric materials designed to take advantage of this temperature sensitivity could have significant commercial applications.

We are only aware of one experimental study that may provide confirmation of our prediction for the temperature dependence of k_0 as given in eq 3.42. Ryan, Macosko, and Bras[23] have carried out SAXS measurements on a model block copolyurethane and made a tentative identification of the ODT. They find the curious result that the peak wavevector decreases rapidly on cooling through the transition region (which they attribute to chain stretching) and then *increases* as the temperature is further lowered in the microphase-separated state. Except for the initial decrease, which cannot be described by the present theory (our RPA-like calculation does not self-consistently account for chain stretching), the increase in k_0 in the ordered phase would seem to be in qualitative agreement with eq 3.42 for a sample with a tendency for alternation $\lambda < \lambda_L$.

Direct visual evidence for the existence of coexisting liquid phases in random copolymer melts comes from the experiments of Stupp and co-workers,[35] where one of the monomer types was mesogenic. In this instance, coexisting nematic and isotropic liquid phases were observed (see also ref 22). Liquid–liquid phase separation has also been observed experimentally and predicted theoretically[21] in *blends* of random copolymers having different compositions and/or sequence distributions. However, such phase separation is less surprising than for the case of a pure random copolymer melt considered here because the distribution of chain compositions is doubly peaked in such blends and the composition difference of the peaks can be of order unity.

Evidence of solid–liquid coexistence (such as that postulated in Figure 6b) is provided by the measurements of Koberstein, Russell, and Leung[36] on segmented polyurethanes. Moreover, there is mounting experimental evidence that microphases with long-range order are very difficult to achieve in segmented copolymer melts with a broad distribution of block lengths,[9,14,23,36-39] consistent with our finding of small or nonexistent free-energy differences between different structures. Carefully prepared alternating multiblocks, however, have been shown to exhibit moderate degrees of long-range order on annealing.[12,13] Finally, we note that microstructural models related to the random wave pattern eq 3.24 have been successfully used to interpret scattering data from microphase-separated polyurethanes and other multiblock copolymers.[14]

Our simple model of random multiblocks has the shortcoming that it does not account for a distribution of overall length, i.e., Q or N. Particularly for short copolymers, phase behavior could be quite sensitive to chain length polydispersity. Even for compositionally monodisperse systems, such as anionically prepared diblock mixtures of constant f, a distribution of N can lead to multiphase coexistence.[40,41] The simultaneous presence of chain length and compositional dispersity could greatly enrich the thermodynamic possibilities, producing phase diagrams and multicritical phenomena even more complex than those addressed in the present paper.

The analysis presented here could be extended in several other directions. For quantitative application of the theory to some experimental systems it may prove necessary to generalize the analysis to monomers with unequal statistical segment lengths or to prepolymers with unequal degrees of polymerization. One might also want to generalize the analysis to rigid-flexible segmented copolymers or to use the free energy derived here as a starting point for studying rheology and dynamics.

Finally, we should comment on the accuracy of the mean-field approximation employed throughout. The approximation is expected to be worst in the vicinity of the two branches of the critical line ($f = {}^1/_2$): $\chi = \chi_s(\lambda)$ for $\lambda > \lambda_L$ and $\chi = \chi_{sm}(\lambda)$ for $\lambda < \lambda_L$, where the osmotic susceptibility is singular. The positive branch corresponds to a conventional liquid–liquid separation, so we expect fluctuation corrections to renormalize this mean-field critical line into a new critical line with $3 - d$ Ising exponents. Since the molecules separating to form the two phases are high molecular weight polymers, however, we expect a very narrow nonclassical region about the critical line that is only N^{-1} wide in reduced temperature.[42] On the negative branch, $\lambda < \lambda_L$, the mean-field transition is second-order and at $k^* \neq 0$. For such transitions, it is believed that composition fluctuations have the effect of inducing a weak first-order phase transition.[2,34,43] Such effects are likely to be important in displacing the actual ODT from the mean-field ODT, particularly far from the Lifshitz point. Precisely at $\lambda = \lambda_L$ the effects of fluctuations are not well understood, however. One possibility is that they renormalize the multicritical exponents. Alternatively, if the lower critical dimension of the isotropic Lifshitz point exceeds 3, the fluctuations might actually suppress the transition to $T = 0$, producing a cusp in the renormalized version of Figure 4. An analysis of fluctuations for the $f = {}^1/_2$, $Q \to \infty$, $\lambda = 0$ special case of random copolymers was recently carried out in ref 27 by means of a self-consistent Hartree approximation. These authors find a fluctuation-induced first-order transition, but we believe this to be inapplicable to the case of finite Q where a finite-width biphasic liquid region exists. Clearly, more detailed studies of fluctuation effects in these complex systems are needed.

Acknowledgment. This work was supported in part by AT&T Bell Laboratories, the Camille and Henry Dreyfus Foundation, The Exxon Education Foundation, and the National Science Foundation under PYI Grant DMR-9057147.

Appendix A: Analysis of Chemical Correlations

In this appendix we discuss a method for computing the correlation functions that characterize the block sequences of the model defined in section II. Since the sequences on different chains are uncorrelated, we restrict consideration to a single multiblock chain with Q segments, each of which can be either of type A or type B. The successive segments on the chain are indexed by an integer l ($1 < l < Q$), and we associate a stationary random variable θ_l with the lth segment that takes the value 1 if the segment is type A and −1 if the segment is type B. The joint probability distribution function, $P(\{\theta_l\})$, describes the distribution of molecular species in the multiblock melt and follows from the Markov model of copolymerization described in section II. Instead of constructing this distribution function, which depends parametrically on f and λ, we focus here on a general method for computing its various moments.

The singlet distribution function, $P_1(\theta_l)$, follows trivially from the fact that θ_l is a stationary random variable:

$$P_1(\theta_l) = f\delta_{\theta_l,1} + (1-f)\delta_{\theta_l,-1} \tag{A.1}$$

Here, δ_{ij} is the Kronecker δ function. From eq A.1 it follows that

$$\langle\theta_l\rangle_{ave} \equiv \sum_{\theta}\theta P_1(\theta) = 2f - 1 \tag{A.2}$$

To compute the higher order moments, it is convenient to introduce a new random variable with zero mean, defined by

$$\sigma_l = \theta_l - \langle\theta_l\rangle_{ave} \tag{A.3}$$

The variable σ_l assumes the values $2(1-f)$ and $-2f$, respectively, if a segment is of type A or type B. Correlation functions of the σ_l variables are easily calculated by a transfer matrix method, which is facilitated by the following definitions:

$$\mathbf{p} = \begin{bmatrix} p_{AA} & p_{AB} \\ p_{BA} & p_{BB} \end{bmatrix} \tag{A.4}$$

$$\mathbf{p}_1 = \begin{bmatrix} f \\ 1-f \end{bmatrix} \tag{A.5}$$

$$\sigma_R = \begin{bmatrix} 2(1-f) & 0 \\ 0 & -2f \end{bmatrix} \tag{A.6}$$

$$\sigma_L = \begin{bmatrix} 2(1-f) \\ -2f \end{bmatrix} \tag{A.7}$$

The physical interpretation of these quantities should be readily apparent. The matrix $\mathbf{p}$ is the matrix of conditional pair probabilities for the occupancy of adjacent segments on a chain. Its various elements were discussed in section II. The column vector $\mathbf{p}_1$ is a vector with elements equal to the probability that a given segment is either of type A or type B. Finally, σ_R and σ_L are a diagonal matrix and a column vector, respectively, with nonvanishing elements equal to the two permisible values of σ_l.

With these definitions, expressions for correlation functions of any order can be written compactly. For example, the pair correlation function of the occupation variables can be written as

$$\langle\sigma_l\sigma_k\rangle_{ave} = \langle\theta_l\theta_k\rangle_{ave} - \langle\theta_l\rangle_{ave}\langle\theta_k\rangle_{ave} = \sigma_L{}^T\mathbf{p}^{|l-k|}\sigma_R\mathbf{p}_1 \tag{A.8}$$

where the superscript T denotes the matrix transpose. In this expression for $l > k$ the vector $\mathbf{p}_1$ gives the initial probability that the kth segment is type A or type B and the matrix σ_R assigns the appropriate value of σ_k. The $l - k$ factors of $\mathbf{p}$ then propagate the probability vector to segment l and the final contraction with the row vector $\sigma_L{}^T$ assigns the appropriate value of σ_l. By inserting a unitary transformation to diagonalize $\mathbf{p}$, evaluation of $\mathbf{p}^{l-k}$ and completion of the matrix algebra in eq A.8 is straightforward. Explicitly performing this algebra and making use of eqs 2.1–2.6 leads to the expression

$$\langle\sigma_l\sigma_k\rangle_{ave} = 4f(1-f)\lambda^{|l-k|} \tag{A.9}$$

which confirms eq 2.10.

Similar expressions can be written for the higher order correlation functions. For example, the third-order correlation function $\langle\sigma_k\sigma_l\sigma_m\rangle_{ave}$ in the case of $k > l > m$ is given by

$$\begin{aligned}\langle\sigma_k\sigma_l\sigma_m\rangle_{ave} &= \sigma_L{}^T\mathbf{p}^{k-l}\sigma_R\mathbf{p}^{l-m}\sigma_R\mathbf{p}_1 \\ &= 8f(1-f)(1-2f)\lambda^{k-l}\lambda^{l-m}\end{aligned} \tag{A.10}$$

which is of order λ^2 for $\lambda \ll 1$. Similarly, the fourth-order correlation function $\langle\sigma_k\sigma_l\sigma_m\sigma_n\rangle_{ave}$ for $k > l > m > n$ is given by

$$\begin{aligned}\langle\sigma_k\sigma_l\sigma_m\sigma_n\rangle_{ave} &= \sigma_L{}^T\mathbf{p}^{k-l}\sigma_R\mathbf{p}^{l-m}\sigma_R\mathbf{p}^{m-n}\sigma_R\mathbf{p}_1 \\ &= 16f(1-f)\lambda^{m-n}\lambda^{k-l}[f(1-f) + (1-2f)^2\lambda^{l-m}]\end{aligned} \tag{A.11}$$

This correlation function is also of order λ^2 for $\lambda \ll 1$. However, it is important to note that $\langle\sigma_k{}^2\sigma_m{}^2\rangle_{ave}$ is of order $\lambda^0 = 1$ for arbitrary k and m.

Appendix B: Derivation of the Landau Free Energy

In this appendix we outline the method used to compute the Landau expansion of the free energy for the multiblock copolymer model defined in section II. Although an approach based on the replica trick is available,[24,25] we employ a simple nonreplica method.[22] Both approaches, however, lead to the same free-energy expression. The fundamental variables of our microscopic theory are the set of monomer positions, $\{\mathbf{R}_i(s)\}$, where $i = 1, 2, ..., N_p$ indexes the various chains in the sample and $s = 1, 2, ..., N$ indexes the *monomers* along a chain. The segment index l is related to s by $l = \text{int}\,(s/M) + 1$. In addition to the monomer positions, we associate with monomer s on chain i an occupation number variable, σ_{il} [note that $l = l(s)$], defined in accordance with eq A.3. If the monomer belongs to a type-A segment, then σ_{il} takes the value $2(1-f)$; alternatively, if the monomer belongs to a type-B segment, then σ_{il} is assigned the value $-2f$.

Having introduced the microscopic variables of concern, we can now write down the expression for the configurational partition function (canonical ensemble) of our model multiblock melt:

$$Z = \int d\{\mathbf{R}\}\,\delta(\phi-1)\,e^{-H_0[\mathbf{R}]+\chi\int d\mathbf{x}\psi^2(\mathbf{x})} \tag{B.1}$$

In this expression, the δ functional $\delta(\phi-1)$ forces the microscopic monomer volume fraction

$$\phi(\mathbf{x}) = \sum_i \sum_s \delta[\mathbf{x}-\mathbf{R}_i(s)] \tag{B.2}$$

to be unity at all points $\mathbf{x}$ in the sample (incompressibility assumption). Here, we continue to work in units where the monomer volume is unity and $k_BT = 1$. The chain configurational entropy (Edwards' Hamiltonian) is given by

$$H_0[\mathbf{R}] = \frac{3}{2b^2}\sum_i \sum_s |\mathbf{R}_i(s) - \mathbf{R}_i(s+1)|^2 \tag{B.3}$$

where b is the statistical segment length (taken to be the same for both types of monomers). Finally, the term $\chi\int d\mathbf{x}\, \psi^2(\mathbf{x})$ describes the energetic preference of similar monomer contacts over dissimilar monomer contacts. The parameter χ is the usual Flory parameter describing the interaction strength between A and B monomers,[30,31] and $\psi(\mathbf{x})$ is a microscopic concentration field defined by

$$\psi(\mathbf{x}) = \frac{1}{2}\sum_i \sum_s \sigma_{il}\delta[\mathbf{x}-\mathbf{R}_i(s)] \tag{B.4}$$

Our motivation for introducing the field $\psi(\mathbf{x})$ is that its expectation value, $m(\mathbf{x})$, when averaged over all realizations of the block sequences, is a useful Landau-type order parameter for investigating the thermodynamic properties of random block copolymer melts.[24,25] In particular, $m(\mathbf{x})$ is defined by

$$m(\mathbf{x}) = \frac{1}{2}\sum_i \sum_s \langle\langle \sigma_{il}\delta[\mathbf{x}-\mathbf{R}_i(s)]\rangle\rangle_{\text{ave}} \tag{B.5}$$

where the inner average $\langle\cdots\rangle$ denotes an ensemble average with a statistical weight given by the integrand of eq B.1 and the outer average $\langle\cdots\rangle_{\text{ave}}$ indicates an average over the $\{\sigma_{il}\}$ variables according to the prescription given in Appendix A. The reason for focusing on the field $m(\mathbf{x})$ is that it is defined to vanish in the case of a single homogenous phase, takes uniform nonzero values in the case of coexisting homogenous phases, and exhibits periodic spatial variations in the case of a mesophase.

In order to express the free energy as a functional of $m(\mathbf{x})$, it proves convenient to rewrite the partition function B.1 in the following way:

$$Z = \int D[m]\, e^{\chi\int d\mathbf{x}\, m^2}\int d\{\mathbf{R}\}\, \delta(1-\phi)\, \delta(m-\psi)\, e^{-H_0[\mathbf{R}]}$$

$$= \int D[m]\, e^{\chi\int d\mathbf{x}\, m^2}\int D[J_\phi]\int D[J_m]\times$$

$$\exp\{i\int d\mathbf{x}\, (J_\phi + J_m m) + G[J_\phi,J_m]\} \tag{B.6}$$

where

$$G[J_\phi,J_m] \equiv \ln\langle \exp[-i\int d\mathbf{x}\, (J_\phi\phi + J_m\psi)]\rangle_0 \tag{B.7}$$

In this final definition, $\langle\cdots\rangle_0$ denotes an ensemble average with statistical weight $\exp(-H_0[\mathbf{R}])$. As the multiblock chains are noninteracting in this ensemble, we can write

$$G[J_\phi,J_m] = \ln\prod_i \langle \exp[-i\int d\mathbf{x}(J_\phi\phi_i + J_m\psi_i)]\rangle_0 \tag{B.8}$$

where ϕ_i and ψ_i are the contributions of chain i to the total fields ϕ and ψ. Equation B.8 can be rewritten as

$$G[J_\phi,J_m] = \sum_i \ln\langle \exp[-i\int d\mathbf{x}(J_\phi\phi_i + J_m\psi_i)]\rangle_0$$

$$= N_p\langle \ln\langle \exp[-i\int d\mathbf{x}(J_\phi\phi_1 + J_m\psi_1)]\rangle_0\rangle_{\text{ave}} \tag{B.9}$$

The latter expression follows from the fact that every chain constitutes an independent realization of the possible multiblock sequences—hence the sum on chains effects a disorder average in the thermodynamic limit.

Our next task is to develop $G[J_\phi,J_m]$ as a Taylor expansion in the fields J_ϕ and J_m, appropriate for cases of weak segregation of the A and B monomers. To facilitate this, it proves convenient to introduce the new fields

$$\tilde{J}_\phi(\mathbf{x}) = J_\phi(\mathbf{x}) - \frac{1}{V}\int d\mathbf{x}\, J_\phi(\mathbf{x})$$

$$\tilde{J}_m(\mathbf{x}) = J_m(\mathbf{x}) - \frac{1}{V}\int d\mathbf{x}\, J_m(\mathbf{x}) \tag{B.10}$$

where V is the system volume. In terms of the "tilde" fields, whose spatial integrals vanish, eq B.9 can be written

$$G[J_\phi,J_m] = -i\int d\mathbf{x}\, J_\phi +$$

$$N_p\langle \ln\langle \exp[-i\int d\mathbf{x}(\tilde{J}_\phi\phi_1 + \tilde{J}_m\psi_1)]\rangle_0\rangle_{\text{ave}} \tag{B.11}$$

where we have used $N_pN/V = 1$ (for unit monomer volume) and $\langle\sigma_l\rangle_{\text{ave}} = 0$ (cf. eq A.3). Next it is convenient to separate $G[J_\phi,J_m]$ as

$$G[J_\phi,J_m] = -i\int d\mathbf{x}\, J_\phi + \tilde{G}[\tilde{J}_\phi,\tilde{J}_m] \tag{B.12}$$

and develop $\tilde{G}[\tilde{J}_\phi,\tilde{J}_m]$ in powers of $\tilde{J}_\phi$ and $\tilde{J}_m$ to order $\tilde{J}_m^4$. As we shall see below, it turns out that the values of $\tilde{J}_\phi$ that contribute to the integral in eq B.6 are of order $\tilde{J}_m^2$. Hence, the required terms in the expansion of $\tilde{G}$ to order $\tilde{J}_m^4$ are

$$\tilde{G}[\tilde{J}_\phi,\tilde{J}_m] = N_p\left\{\frac{1}{2}\langle\langle\epsilon_\phi^2\rangle_0\rangle_{\text{ave}} + \frac{1}{2}\langle\langle\epsilon_m^2\rangle_0\rangle_{\text{ave}} + \right.$$

$$\frac{1}{3!}\langle\langle\epsilon_m^3\rangle_0\rangle_{\text{ave}} + \frac{1}{2}\langle\langle\epsilon_\phi\epsilon_m^2\rangle_0\rangle_{\text{ave}} + \frac{1}{4!}[\langle\langle\epsilon_m^4\rangle_0\rangle_{\text{ave}} -$$

$$\left. 3\langle\langle\epsilon_m^2\rangle_0^2\rangle_{\text{ave}}]\right\} \tag{B.13}$$

where

$$\epsilon_\phi \equiv -i\int d\mathbf{x}\, \tilde{J}_\phi\phi_1$$

$$\epsilon_m \equiv -i\int d\mathbf{x}\, \tilde{J}_m\psi_1 \tag{B.14}$$

The quantities on the right-hand side of eq B.13 can be evaluated by performing the indicated Gaussian single-chain averages over $\mathbf{R}_1(s)$ and disorder averages over σ_{1l} according to the method of Appendix A. (In the following we will drop the index 1 on the chain of concern.) In carrying out the latter type of average, it turns out that the correlation functions of the σ_l variables are required to fourth order. These have been calculated in Appendix A, but the expressions that arise for some of the terms in eq B.13 are quite unwieldy for general values of λ. To simplify the calculations, we have evaluated the cubic and quartic terms in eq B.13 only to first order in λ, essentially restricting consideration to the case of weak chemical

correlations along the chain. This restriction, however, is not particularly severe since qualitative changes in phase behavior due to strong correlations are only manifest when λ is within $1/Q$ of +1 or −1. Such extreme values of λ can generally not be achieved in realistic copolymer systems. A second approximation that we invoke in evaluating the terms in eq B.13 is to coarse-grain the higher order terms over a scale $R_M^2 = Mb^2/6$, the radius of gyration of a single segment. This is achieved by recognizing that the Fourier coefficients of the $\tilde{J}_\phi$ and $\tilde{J}_m$ fields with wavevectors $k \ll 1/R_M$ provide the principal contribution to the free energy of a mesophase close to the ODT or of coexisting homogenous phases. Hence, in the cubic and quartic terms of eq B.13 we replace all coefficients of $\tilde{J}_\phi$ or $\tilde{J}_m$ that are functions of kR_M by their limiting values for zero argument. The quadratic terms (first two on the right-hand side of eq B.13) are evaluated without using the above approximations in order to preserve the exact mean-field spinodal. Finally, we note that long multiblock chains are assumed, i.e., $Q \gg 1$. Subdominant terms in Q are dropped throughout.

The terms in eq B.13 are most conveniently expressed as functionals of the Fourier coefficients of the $\tilde{J}_\phi$ and $\tilde{J}_m$ fields. These coefficients (transforms in the thermodynamic limit) are defined by, e.g., for $\tilde{J}_\phi$

$$\tilde{J}_\phi(\mathbf{k}) = \int d\mathbf{x}\, e^{i\mathbf{k}\cdot\mathbf{x}} J_\phi(\mathbf{x}) \tag{B.15}$$

The quadratic terms in eq B.13 evaluate to the compact expressions

$$\frac{N_p}{2}\langle\langle \epsilon_\phi^{\,2}\rangle_0\rangle_{\text{ave}} = -\frac{1}{2V}\sum_{\mathbf{k}} \tilde{J}_\phi(-\mathbf{k})\, \tilde{J}_\phi(\mathbf{k})\, N g(k^2 R_N^{\,2}) \tag{B.16}$$

$$\frac{N_p}{2}\langle\langle \epsilon_m^{\,2}\rangle_0\rangle_{\text{ave}} = -\frac{1}{2V}\sum_{\mathbf{k}} \tilde{J}_m(-\mathbf{k})\, \tilde{J}_m(\mathbf{k})\, G_2(k^2 R_M^{\,2}) \tag{B.17}$$

where $g(x)$ is the familiar Debye function[30]

$$g(x) \equiv 2[x - 1 + \exp(-x)]/x^2 \tag{B.18}$$

and $R_N^2 = Nb^2/6$ is the overall unperturbed radius of gyration of a multiblock chain. The function $G_2(x)$ that appears in eq B.17 is defined by

$$G_2(x) = C_2 M\left[g(x) + \frac{2\lambda h(x)}{1 - \lambda\exp(-x)}\right] \tag{B.19}$$

where $h(x)$ is a second Debye-like function defined by

$$h(x) = [1 - \exp(-x)]^2/x^2 \tag{B.20}$$

and $C_2 \equiv f(1-f)$.

The cubic terms, which have been simplified by using the approximations described above, are given by

$$\frac{N_p}{3!}\langle\langle \epsilon_m^{\,3}\rangle_0\rangle_{\text{ave}} = \frac{i}{3!}(1 + 6\lambda) C_3 C_2 \frac{M^2}{V^2}\sum_{\mathbf{k}_1}\sum_{\mathbf{k}_2} \times \tilde{J}_m(-\mathbf{k}_1)\, \tilde{J}_m(-\mathbf{k}_2)\, \tilde{J}_m(\mathbf{k}_1 + \mathbf{k}_2) \tag{B.21}$$

$$\frac{N_p}{2}\langle\langle \epsilon_\phi \epsilon_m^{\,2}\rangle_0\rangle_{\text{ave}} = \frac{i}{2}(1 + 2\lambda) C_2 \frac{MN}{V^2}\sum_{\mathbf{k}_1}\sum_{\mathbf{k}_2} \times \tilde{J}_\phi(-\mathbf{k}_1)\, \tilde{J}_m(-\mathbf{k}_2)\, \tilde{J}_m(\mathbf{k}_1 + \mathbf{k}_2)\, g(k_1^{\,2} R_N^{\,2}) \tag{B.22}$$

where $C_3 \equiv (1 - 2f)$.

Finally, we turn to the quartic terms, the first of which can be written as

$$\frac{N_p}{4!}\langle\langle \epsilon_m^{\,4}\rangle_0\rangle_{\text{ave}} = \frac{1}{4!}(1 + 4\lambda) C_2^{\,2} \frac{M^2 N}{V^3}\sum_{\mathbf{k}_1}\sum_{\mathbf{k}_2}\sum_{\mathbf{k}_3} \times \tilde{J}_m(-\mathbf{k}_1)\, \tilde{J}_m(-\mathbf{k}_2)\, \tilde{J}_m(-\mathbf{k}_3)\, \tilde{J}_m(\mathbf{k}_1 + \mathbf{k}_2 + \mathbf{k}_3)\, [g(|\mathbf{k}_1 + \mathbf{k}_2|^2 R_N^{\,2}) + g(|\mathbf{k}_1 + \mathbf{k}_3|^2 R_N^{\,2}) + g(|\mathbf{k}_2 + \mathbf{k}_3|^2 R_N^{\,2})] \tag{B.23}$$

where we have again taken $k_i R_M \ll 1$, retained terms only to first order in λ, and dropped subdominant terms in Q. The final quartic term in eq B.13 evaluates to

$$N_p \frac{3}{4!}\langle\langle \epsilon_m^{\,2}\rangle_0^{\,2}\rangle_{\text{ave}} = (1 + 4\lambda) C_2^{\,2} \frac{M^2 N}{8V^3}\sum_{\mathbf{k}_1}\sum_{\mathbf{k}_2} \times \tilde{J}_m(\mathbf{k}_1)\, \tilde{J}_m(-\mathbf{k}_1)\, \tilde{J}_m(\mathbf{k}_2)\, \tilde{J}_m(-\mathbf{k}_2)\, [1 + 2g(k_1^{\,2} R_N^{\,2} + k_2^{\,2} R_N^{\,2})] \tag{B.24}$$

Our next step is to perform the functional integrals over the J_ϕ and J_m fields in eq B.6. This cannot be done exactly, but within *mean-field theory* these integrals are evaluated by finding the saddle-point Fourier coefficients $J_\phi(\mathbf{k})$ and $J_m(\mathbf{k})$. To this end, we rewrite eq B.6 as

$$Z = \int D[m]\, e^{\chi\int d\mathbf{x}\, m^2} \int D[J_\phi] \int D[J_m]\, \exp\{i\int d\mathbf{x}\, J_m m + \tilde{G}[\tilde{J}_\phi, \tilde{J}_m]\} \tag{B.25}$$

and for the purpose of calculating the saddle-point coefficients, note the following identity:

$$\frac{\delta}{\delta J_\phi(\mathbf{k})} = \frac{\delta}{\delta \tilde{J}_\phi(\mathbf{k})} - \delta_{\mathbf{k},0}\frac{\delta}{\delta \tilde{J}_\phi(0)} \tag{B.26}$$

A similar expression can be written for the derivative $\delta/\delta J_m(\mathbf{k})$.

The saddle-point equation for $\tilde{J}_\phi(\mathbf{k})$ can be written as

$$\frac{\delta \tilde{G}}{\delta J_\phi(-\mathbf{k})} = \frac{\delta \tilde{G}}{\delta \tilde{J}_\phi(-\mathbf{k})} - \delta_{\mathbf{k},0}\frac{\delta \tilde{G}}{\delta \tilde{J}_\phi(0)} = 0 \tag{B.27}$$

which leads to

$$\tilde{J}_\phi(\mathbf{k}) = \frac{i}{2}(1 - \delta_{\mathbf{k},0})(1 + 2\lambda) C_2 \frac{M}{V}\sum_{\mathbf{k}_1} \tilde{J}_m(-\mathbf{k}_1)\, \tilde{J}_m(\mathbf{k} + \mathbf{k}_1) \tag{B.28}$$

In deriving this expression we have used the result $\tilde{J}_\phi(\mathbf{k})$ $\delta_{\mathbf{k},0} = 0$, which follows from the definition B.10. We also note that eq B.28 shows that $\tilde{J}_\phi \sim \tilde{J}_m^{\,2}$ as previously assumed. Substitution of this expression for $\tilde{J}_\phi$ into eq B.13 yield terms of order $\tilde{J}_m^{\,4}$ that exactly cancel the fifth term on the right-hand side of eq B.13 and part of the sixth term. The resulting expression for the partition function is given by

$$Z = \int D[m]\, e^{\chi\int d\mathbf{x}\, m^2} \int D[J_m]\, \exp\left\{\frac{i}{V}\sum_{\mathbf{k}} J_m(-\mathbf{k})\, m(\mathbf{k}) + \frac{N_p}{2}\langle\langle \epsilon_m^{\,2}\rangle_0\rangle_{\text{ave}} + \frac{N_p}{3!}\langle\langle \epsilon_m^{\,3}\rangle_0\rangle_{\text{ave}} - (1 + 4\lambda) C_2^{\,2} \frac{M^2 N}{4V^3}\sum_{\mathbf{k}_1}\sum_{\mathbf{k}_2} \tilde{J}_m(\mathbf{k}_1)\, \tilde{J}_m(-\mathbf{k}_1)\, \tilde{J}_m(\mathbf{k}_2)\, \tilde{J}_m(-\mathbf{k}_2) \times g(k_1^{\,2} R_N^{\,2} + k_2^{\,2} R_N^{\,2})\right\} \tag{B.29}$$

Next, we evaluate the J_m integral by saddle points, again invoking eq B.26 and dropping terms at each order in J_m

that are subddominant in Q. The final result for the partition function can be written

$$Z = \int D[m]\, e^{-H[m]} \tag{B.30}$$

where the "effective Hamiltonian" $H[m]$ is given to fourth order in $m(\mathbf{k})$ by

$$H[m] = \frac{1}{2!V}\sum_{\mathbf{k}} m(\mathbf{k})\, m(-\mathbf{k})\, [G_2^{-1}(k^2R_M^2) - 2\chi] - \frac{C_3}{3!C_2^2MV^2}\sum_{\mathbf{k}_1}\sum_{\mathbf{k}_2} m(\mathbf{k}_1)\, m(\mathbf{k}_2)\, m(-\mathbf{k}_1-\mathbf{k}_2) + \frac{N}{4(C_2M\Lambda)^2V^3}\sum_{\mathbf{k}_1}\sum_{\mathbf{k}_2} m(\mathbf{k}_1)\, m(-\mathbf{k}_1)\, m(\mathbf{k}_2)\, m(-\mathbf{k}_2) \times g(k_1^2R_N^2 + k_2^2R_N^2) \tag{B.31}$$

In obtaining eq B.31, we have replaced factors of $G_2^{-1}(k^2R_M^2)$ in the cubic and quartic terms by the zero wavevector limit of eq B.19

$$G_2^{-1}(0) = (C_2M\Lambda)^{-1} \tag{B.32}$$

which is consistent with our restriction to $k^2R_M^2 \ll 1$. Here, the dimensionless parameter Λ is related to λ by

$$\Lambda = \frac{1+\lambda}{1-\lambda} \tag{B.33}$$

We have also replaced factors of $1 + 4\lambda$ and $1 + 6\lambda$ by factors of Λ^2 and Λ^3, respectively, which are equivalent to $O(\lambda)$.

The final step in our calculation is simply to recognize that within mean-field theory we can use the effective Hamiltonian $H[m]$ as a free energy functional;[34] hence, $F[m] = H[m]$.

References and Notes

(1) See, e.g.: *Developments in Block Copolymers*; Goodman, I., Ed.; Applied Sciences: New York, 1982 and 1985; Vols. 1 and 2.
(2) Bates, F. S.; Fredrickson, G. H. *Annu. Rev. Phys. Chem.* **1990**, *41*, 525.
(3) Bates, F. S. *Science* **1991**, *251*, 898.
(4) Ajdari, A.; Leibler, L. *La Recherche* **1991**, *22*, 732.
(5) Thomas, E. L.; Anderson, D. C.; Henkee, C. S.; Hoffman, D. *Nature* **1988**, *334*, 598.
(6) de Gennes, P.-G. *Faraday Discuss. Chem. Soc.* **1979**, *68*, 96.
(7) Kavassalis, T. A.; Whitmore, M. D. *Macromolecules* **1991**, *24*, 5340.
(8) Benoit, H.; Hadziioannou, G. *Macromolecules* **1988**, *21*, 1449.
(9) Zielinski, J. M.; Spontak, R. J. *Macromolecules*, in press.
(10) Krause, S. *Macromolecules* **1970**, *3*, 85.
(11) Mayes, A. M.; Olvera de la Cruz, M. *J. Chem. Phys.* **1989**, *91*, 7228.
(12) Patel, N. M.; Dwight, D. W.; Hedrick, J. L.; Webster, D. C.; McGrath, J. E. *Macromolecules* **1988**, *21*, 2689.
(13) Dwight, D. W.; McGrath, J. E.; Riffle, J. S.; Smith, S. D.; York, G. A. *J. Electron Spectrosc. Relat. Phenom.* **1990**, *52*, 457.
(14) Samseth, J.; Mortensen, K.; Burns, J. L.; Spontak, R. J. *J. Appl. Polym. Sci.*, in press.
(15) Leibler, L. *Macromolecules* **1980**, *13*, 1602.
(16) Almdal, K.; Rosedale, J. H.; Bates, F. S.; Wignall, G. D.; Fredrickson, G. H. *Phys. Rev. Lett.* **1990**, *65*, 1112.
(17) Bates, F. S.; Rosedale, J. H.; Fredrickson, G. H. *J. Chem. Phys.* **1990**, *92*, 6255.
(18) Rosedale, J. H.; Bates, F. S. *Macromolecules* **1990**, *23*, 2329.
(19) Semenov, A. N. *Sov. Phys. JETP* **1985**, *61*, 733.
(20) Helfand, E.; Wasserman, Z. R. In *Developments in Block Copolymers*; Goodman, I., Ed.; Applied Sciences: New York, 1982; Vol. 1.
(21) Scott, R. *J. Polym. Sci.* **1952**, *9*, 423. Balazs, A. C.; Sanchez, I. C.; Epstein, I. R.; Karasz, F. E.; MacKnight, W. J. *Macromolecules* **1985**, *18*, 2188. Van Hunsel, J.; Balazs, A. C.; Koningsveld, R.; MacKnight, W. J. *Macromolecules* **1988**, *21*, 1528.
(22) Fredrickson, G. H.; Leibler, L. *Macromolecules* **1990**, *23*, 531.
(23) Koberstein, J. T.; Russell, T. P. *Macromolecules* **1986**, *19*, 714. Leung, L. M.; Koberstein, J. T. *Macromolecules* **1986**, *19*, 706. Ryan, A. J.; Macosko, C. W.; Bras, W., preprint.
(24) Shakhnovich, E. I.; Gutin, A. M. *J. Phys. (Fr.)* **1989**, *50*, 1843.
(25) Fredrickson, G. H.; Milner, S. T. *Phys. Rev. Lett.* **1991**, *67*, 835.
(26) Panyukov, S. V.; Kuchanov, S. I. *Sov. Phys. JETP* **1991**, *72*, 368.
(27) Dobrynin, A. V.; Erukhimovich, I. Y. *Sov. Phys. JETP, Lett.* **1991**, *53*, 570.
(28) Odian, G. *Principles of Polymerization*; Wiley-Interscience: New York, 1981.
(29) Hoel, P. G.; Port, S. C.; Stone, C. J. *Introduction to Stochastic Processes*; Houghton Mifflin: Boston, 1972.
(30) de Gennes, P.-G. *Scaling Concepts in Polymer Physics*; Cornell University Press: Ithaca, NY, 1979.
(31) In practical application of the formulas derived here, some account should be taken for the fact that the χ parameter has entropic and nonlocal contributions. See, e.g.: Schweizer, K. S.; Curro, J. G. *Phys. Rev. Lett.* **1988**, *60*, 809.
(32) Hornreich, R. M.; Luban, M.; Shtrikman, S. *Phys. Rev. Lett.* **1975**, *35*, 1678.
(33) Broseta, D.; Fredrickson, G. H. *J. Chem. Phys.* **1990**, *93*, 2927.
(34) Fredrickson, G. H.; Helfand, E. *J. Chem. Phys.* **1987**, *87*, 697.
(35) Moore, J. S.; Stupp, S. I. *Macromolecules* **1988**, *21*, 1217.
(36) Koberstein, J. T.; Russell, T. P. *Macromolecules* **1986**, *19*, 714. Leung, L. M.; Koberstein, J. T. *Macromolecules* **1986**, *19*, 706.
(37) Li, C.; Goodman, S. L.; Albrecht, R. M.; Cooper, S. L. *Macromolecules* **1988**, *21*, 2367.
(38) Wilkes, G. L.; Tayagi, D. *Polymn. Eng. Sci.* **1986**, *26*, 1371.
(39) Ogata, S.; Kakimoto, M.; Imai, Y. *Macromolecules* **1985**, *18*, 851.
(40) Almdal, K.; Rosedale, J. H.; Bates, F. S. *Macromolecules* **1990**, *23*, 4336.
(41) Leibler, L.; Benoit, H. *Polymer* **1981**, *22*, 195.
(42) de Gennes, P.-G. *J. Phys. (Paris)* **1977**, *38*, L-441.
(43) Brazovskii, S. *Sov. Phys. JETP* **1975**, *41*, 85.